Infrared Spectra of Matrix-Isolated [OC···X_2] and [CO···X_2] Complexes (X = Cl, Br) and ab Initio Calculations

A. Schriver,[†] L. Schriver-Mazzuoli,*[,†] P. Chaquin,[‡] and M. Bahou[†]

Laboratoire de Physique Moléculaire et Applications,[§] Unité propre du CNRS 136, Université Pierre et Marie Curie, Tour 13, case 76, 4 place Jussieu, 75252 Paris Cedex 05, France, and Laboratoire de Chimie Théorique, CNRS UMR 7616 and Université Pierre et Marie Curie, Tour 22, case 137, 4 place Jussieu, 75252 Paris Cedex 05, France

Received: December 11, 1998; In Final Form: February 16, 1999

Co-deposition of argon or nitrogen dilute samples of natural and isotopic carbon monoxide and halogen molecules (Cl_2, Br_2, BrCl) produced new narrow absorptions lines assigned to X_2···CO complexes. With BrCl, in an argon matrix two 1:1 complexes were observed, one stronger than the Br_2···CO complex, the other one weaker than the Cl_2···CO complex. In the nitrogen matrix, one complex was only observed, namely, the ClBr···CO complex. For all complexes, observed shifts were larger in nitrogen than in argon matrices and similar to available gas-phase results for Cl_2···CO and Br_2···CO complexes. Irradiation of the samples with a filtered xenon lamp ($\lambda > 360$ nm) induced in an argon matrix (not in a nitrogen matrix) the isomerization of the complexes into a metastable form CO···X_2 identified for the first time. Back isomerization was observed by weak temperature increase. The structure and energetics of the four complexes formed between CO and BrCl were investigated by DFT ab initio calculations and compared to complexes formed between CO and Cl_2 and Br_2.

1. Introduction

Weakly bonded complexes containing a CO molecule have attracted special interest because carbon monoxide can act as a weak π Lewis acid or as a base donating σ electron density.[1,2] In the latter case, complex formation can involve either the carbon or the oxygen atom as predicted by theoretical calculations:[3−5] OC···X_2 (form 1) CO···X_2 (form 2).

From experimental results in complex 1 (donating charge from the carbon side) the frequency of ν(CO) is expected to increase and in complex 2 (donating charge from the oxygen side) to decrease compared to the value for the isolated CO molecule. CO complexes with HX (X = F, Cl, Br, I) have been extensively studied by gas spectroscopy[6−10] and by infrared matrix spectroscopy.[11,12] Recently, high-resolution rovibrational absorption spectroscopy of OC···Cl_2[13] and OC···Br_2[14] complexes have been recorded. The complexes were found to be linear with Cl_2 or Br_2 acting as σ electron acceptors and CO as electron donor from the carbon atom. An ab initio study of the CO···Cl_2 complex[15] showed minima especially for two linear structures CO···Cl_2 and OC···Cl_2 with the latter (only observed experimentally) more stable than the former.

The matrix isolation technique (MIT) is known to be an effective means for studying van der Waals complexes despite matrix effects, which can play a role in the properties of the complexes. In particular, the MIT can trap a complex in both structural forms, preventing rearrangement of the less stable into the more stable structural form as recently evidenced for the CO···CO_2 system.[16] Furthermore, the photochemistry of small molecules in a rare-gas solid can inhibit the migration of photofragments, and recombination in the matrix cage can lead to two different complex forms. As a matter of fact, the molecular complexes OC···HF and CO···HF have been selectively formed in high yield by UV photofragmentation of matrix-isolated formyl fluoride.[12]

The present paper reports both experimental results concerning Cl_2/CO, Br_2/CO, and BrCl/CO mixtures trapped both in argon and in nitrogen matrices and ab initio calculations on the halogen carbon monoxide interactions. Our aim in this study was twofold: first, to obtain a more complete picture of the CO···X_2 complexes including ^{18}O- and ^{13}C-enriched CO and BrCl molecules; second, to isolate and characterize experimentally and theoretically the second isomer (form 2) by irradiation of the matrix.

2. Experimental Section

CO (Air Liquide N47), Ar (Air Liquide N56), N_2 (Air Liquide N50), and ^{13}CO (Eurisotop, 99.95%) were used without further purification. $^{12}C^{18}O$ was prepared in low yield by discharge of a mixture of $^{18}O_2$ and $C^{16}O$ followed by distillation of $C^{18}O$ at −180 °C. Cl_2 (supplied from Matheson, 99.9%) and Br_2 (supplied from Fluka, 99%) were distilled and degassed before use. Gas mixtures were prepared by standard manometric techniques on a grease-free vacuum line. BrCl was obtained by mixing bromine vapor with chlorine gas, leading to an equilibrium among BrCl, Cl_2, and Br_2. Matrix samples were prepared on a gold-plated copper block maintained at 20 K for Ar and 17 K for N_2 by a closed-cycle helium refrigerator (Air Product Displex model 202 A). The deposition rate was about 10 mmol/h. A double injection was used, one for carbon monoxide, the other one for halogen molecules. Chosen concentrations varied from 1/500 to 1/200 for halogen species and from 1/10000 to 1/1000 for carbon monoxide.

The spectra were recorded in reflection mode at 11 K on a Bruker 113v spectrophotometer with a nominal resolution of

* To whom correspondence should be addressed.
[†] Laboratoire de Physique Moléculaire et Applications.
[‡] Laboratoire de Chimie Théorique.
[§] Laboratoire Associé aux Universités P. et M. Curie.

10.1021/jp984719t CCC: $18.00
Published on Web 03/30/1999

0.1 and 0.04 cm^{-1}. Irradiation was carried out at 11 K with a xenon lamp (150 W) and a 360 nm filter cutoff.

3. Calculation Methods

The Gaussian 94 series of programs[17] has been used throughout this work. Previous studies have shown that DFT methods afford good geometrical parameters and vibration frequencies in a series of XYO compounds[18] and NOX (X, Y reperesent halogens) isomers[19] but sometimes poorly reliable energies. Reliable energy parameters require extensive treatment of the correlation, for example by CCSD(T) method,[20] wasting computational time, together with large basis sets. A good compromise is thus to calculate vibration frequencies and geometrical parameters at the DFT level and then to perform a single-point calculation at the CCSD(T) level. Becke's three-parameter functional[21] with the correlation functional of Lee, Yang, and Paar[22] (B3LYP) has been used. This functional has been successfully used in calculating dihalogen···ozone complexes.[18] Moreover, a satisfactory agreement is found with previous calculations of $COCl_2$ complexes[13] at the MP2 level. The basis set is derived from Ahlrichs[23] by adding 2d and 1f AOs on carbon, oxygen, and chlorine (carbon: $\alpha_d = 1.097$ and 0.318, $\alpha_f = 0.761$; oxygen: $\alpha_d = 2.314$ and 0.645, $\alpha_f = 1.428$; chlorine: $\alpha_d = 1.072$ and 0.357, $\alpha_f = 0.706$) and 1f on bromine ($\alpha_f = 0.55$), yielding the following contraction scheme: C and O, 11s6p2d1f/5s3p2d1f; Cl, 14s8p1d1f/5s4d2d1f; Br, 17s13p6d1f/6s5p2d1f. A rough estimation of BSSE corrections has been performed using the ghost atom method; the energy of each moiety has been calculated in the presence of the AOs' second entity with a zero nuclear charge.

4. Spectrum of Monomeric CO

Carbon monoxide was examined at high dilution in argon and nitrogen matrices without co-deposited halogen molecules. In argon matrices, as previously reported,[24,25] the monomeric CO band is characterized by a line at 2138.5 cm^{-1}, which shows a reversible broadening when the temperature is raised. The low-frequency shoulder at 2136.6 cm^{-1} that appears on the monomer absorption peak in argon was assigned to the CO dimer by Diem et al.[25] In the nitrogen matrix monomeric CO absorbs at 2139.8 cm^{-1} without significant temperature dependence, indicating that there is no librational motion of CO in the matrix cage. With a resolution of 0.1 cm^{-1}, the full width at half-maximum (fwhm) of the CO absorption at 11 K is equal to 0.2 cm^{-1} in nitrogen, whereas in argon, it is equal to 1.8 cm^{-1}.

In parallel experiments with 70% $^{12}C^{18}O$ and 99% ^{13}CO-enriched CO, the $C^{18}O$ monomer absorption appeared at 2087.3 cm^{-1} in argon and the ^{13}CO absorptions were measured to be 2091.3 and 2088.7 cm^{-1} in argon and nitrogen, respectively.

The CO spectrum in argon and in nitrogen is extremely sensitive to the presence of impurities as H_2O and CO_2. Traces of water in argon matrices cause the appearance of a doublet at 2149.2 and 2148.2 cm^{-1},[26] while in nitrogen the binary complex is observed as a single band measured to 2147.5 cm^{-1}.[27] In the presence of CO_2, the CO band gets three satellites in the argon matrix at 2139.38, 2140.04, and 2140.23 cm^{-1} [16] and four satellites in nitrogen matrix at 2138.07, 2138.86, 2140.80, and 2141.57 cm^{-1}.[27]

5. Spectroscopic Identification of OC···X$_2$ Complexes (Form 1)

5.1. Argon Matrix. *CO···Cl$_2$.* Some experiments were conducted with CO and Cl_2 in solid argon using different reagent concentrations. In an experiment using intermediate concentrations (co-deposition of Cl_2/Ar (1/500), and CO/Ar (1/1000)) the spectrum displayed in Figure 1 (trace a) showed CO monomer absorption and bands due to interaction between CO and Cl_2. New product absorptions consisted of a strong narrow band at 2140.6 cm^{-1} (fwhm = 0.2 cm^{-1}) and a weak satellite at 2139.4 cm^{-1}. No band due to the perturbed Cl_2 molecule was observed in the 600−500 cm^{-1} region. Warming the matrix produced many changes in the spectrum as illustrated in Figure 1 (traces b and c). At 35 K the CO monomer band decreased with the appearance of two weak features at 2139.2 and 2139.8 cm^{-1}. The intensity of the 2140.6 and 2139.4 cm^{-1} bands remained constant. Annealing at 40 K reduced the intensity of the main band with respect to the freshly deposited matrix; the 2139.4 cm^{-1} feature disappeared and absorptions at 2139.2 and 2139.8 cm^{-1} grew markedly with the appearance of a triplet at 2143.1, 2143.8, and 2144.6 cm^{-1}. With a more diluted CO sample (CO/Ar: 1/10000) and the same concentration in Cl_2 (Cl_2/Ar: 1/500) (trace d), the band at 2140.6 cm^{-1} with a satellite at 2139.4 cm^{-1} was again present. At this CO dilution, the CO monomer absorption did not appear.

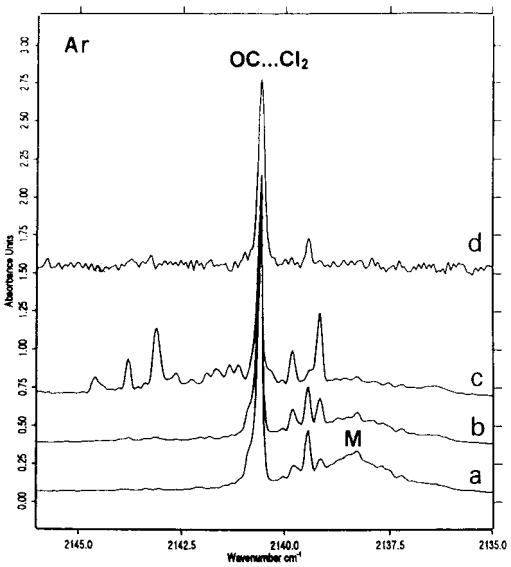

Figure 1. Infrared spectra in the ν(CO) spectral region of an argon matrix containing CO and Cl_2 recorded at 11 K: (a) CO/Cl_2/Ar = 1/2/2000 after deposition at 20 K; (b) the same sample after annealing at 30 K; (c) the same sample after annealing at 40 K; (d) CO/Cl_2/Ar = 1/10/10000 after deposition at 20 K.

The two bands at 2140.6 and 2139.4 cm^{-1} for which the relative intensity after deposition ($I_{2140.6}/I_{2139.4} = 10.5$) was not affected by different concentrations of reagents in the matrix, are assigned to the 1:1 complex formed between CO and Cl_2. The weak satellite at 2139.4 cm^{-1}, which appears at 1 cm^{-1} below the main CO band in the complex, is probably due to a different trapping environment. The blue shift in the CO stretching frequency as observed in the gas phase confirms that in the complex the carbon acts as a base donating σ electron density.

Experiments at high dilution in two reagents were also performed with isotopically substituted carbon monoxide. Co-deposition of $^{13}CO/^{12}CO$/Ar (99% ^{13}CO) and Cl_2/Ar provided similar results as described above. A band at 2093.4 cm^{-1} was observed in the ^{13}CO region. In the corresponding experiments with $C^{16}O/C^{18}O$ mixtures the product absorptions in the $C^{16}O$ were present again and a new product absorption appeared at 2089.5 cm^{-1} in the $C^{18}O$ region.

TABLE 1: Absorptions (cm^{-1}) Observed for the CO Monomer (Natural and Isotopic) and the Perturbed CO Mode in $Cl_2\cdots CO$, $Br_2\cdots CO$, $BrCl\cdots CO$, and $ClBr\cdots CO$ Complexes Trapped in Argon and Nitrogen Matrices

	argon			nitrogen	
	$^{12}C^{16}O$	$^{13}C^{16}O$	$^{12}C^{18}O$	$^{12}C^{16}O$	$^{13}C^{16}O$
CO	2138.5	2091.3	2087.3	2139.8	2088.7
$Cl_2\cdots CO$	2140.6	2093.4	2089.5	2148.5	2101.0
$Br_2\cdots CO$	2143.9	2096.7	2092.9	2152.5	2105.3
$BrCl\cdots CO$	2138.0_5	2090.9	2087.0		
$ClBr\cdots CO$	2147.9_5	2100.6	2096.8_5	2156.9	2109.6

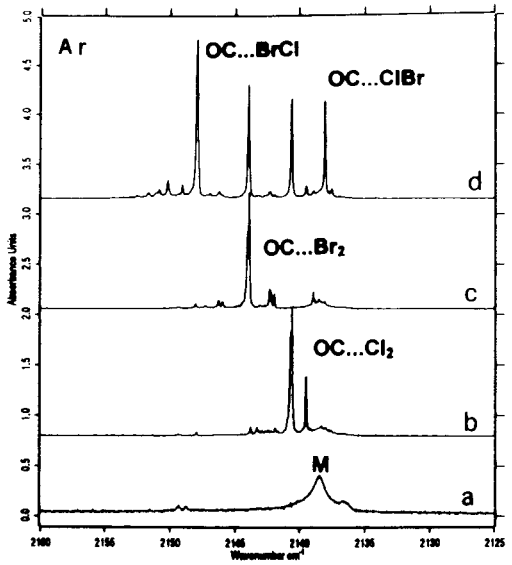

Figure 2. Comparison between IR spectra after deposition in the CO spectral region: (a) CO/Ar = 1/1000 mixture; (b) $CO/Cl_2/Ar$ = 1/10/10000 mixture; (c) $CO/Br_2/Ar$ = 1/10/10000 mixture; (d) $CO/Cl_2 + Br_2/Ar$ = 1/10 + 10/10000 mixture.

In all experiments, the strong absorption characteristic of the $OC\cdots Cl_2$ complex appeared as a single band even at high resolution (0.04 cm^{-1}). No splitting in the CO submolecule absorption due to isotopic Cl_2 submolecule was observed.

The new weak bands observed after temperature effects probably belong to aggregates with a larger stoichiometry. Complementary experiments are needed to identify accurately these aggregates; however, it is not the topic of the present work.

Table 1 summarizes the band frequencies of the 1:1 complexes involving natural and isotopic carbon monoxide.

CO/Br₂. A set of experiments was performed with high dilution CO/Ar sample (1/10000) and more concentrated Br_2/Ar sample (1/500). As shown in Figure 2 (trace c), a new CO absorption due to the $OC\cdots Br_2$ complex appeared at 2143.9 cm^{-1} with in addition a satellite band at 2143.1 cm^{-1} due to site splitting. The CO monomer absorption was not observed. Corresponding experiments with a $^{13}CO/^{12}CO$ mixture and a $C^{18}O/C^{16}O$ mixture provided results comparable to those with $^{12}C^{16}O$. The major product band positions were observed at 2096.7 and 2092.9 cm^{-1} respectively.

CO/BrCl. When CO/Ar (1/10000) and equilibrated $Br_2 + Cl_2$/Ar (1/200) were condensed, four new features that did not belong to the CO monomer absorption (not observed) appeared in the ν_{CO} region as illustrated Figure 2 (trace d). The absorptions at 2140.6 and 2143.9 cm^{-1} were previously observed in experiments described above, and they characterized the perturbed ν(CO) mode of the carbon monoxide submolecule in the interaction with Cl_2 and Br_2, respectively. The other bands at 2147.9 and 2138.05 cm^{-1} are clearly due to new complexes between carbon monoxide and BrCl. Two complexes can be expected: ($OC\cdots BrCl$), in which carbon monoxide is bound to BrCl via the bromine atom, and ($OC\cdots ClBr$), in which CO is bound to BrCl via the chlorine atom. On the basis of the observed CO shifts due to interaction with Cl_2 and Br_2, the band located at 2147.9 cm^{-1} was assigned to the $OC\cdots BrCl$ 1:1 complex and the other one measured at 2138.05 cm^{-1} to the $OC\cdots ClBr$ complex, a conclusion supported by ab initio calculations reported below.

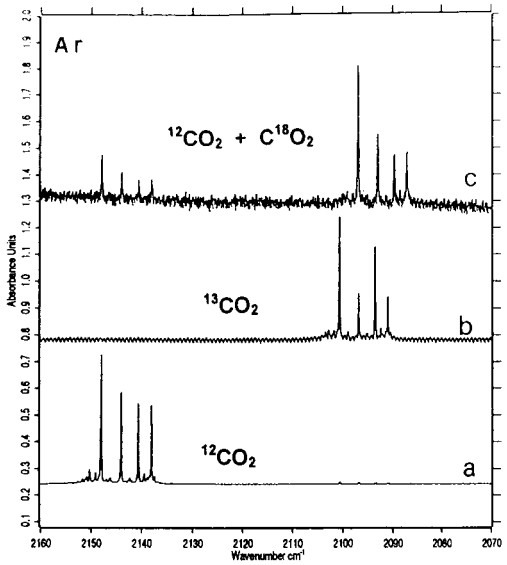

Figure 3. Infrared spectra in the ν(CO) spectral region of bromine−chloride−carbon monoxide samples recorded at 11 K with a resolution of 0.1 cm^{-1}: (a) $^{12}C^{16}O/Cl_2 + Br_2/Ar$ = 1/10 + 10/10000 mixture; (b) $^{13}C^{16}O/Cl_2 + Br_2/Ar$ = 1/10 + 10/10000 mixture; (c) $^{12}C^{18}O/Cl_2 + Br_2/Ar$ = 1/10 + 10/10000 mixture.

Co-deposition of $^{13}C^{16}O$ and $Br_2 + Cl_2$ in a double-jet experiment gave a set of absorptions similar to those with $^{12}C^{16}O$. Absorptions due to ^{13}CO in the interaction with BrCl and ClBr were measured at 2100.6 and 2090.9 cm^{-1}. Isotopic $^{12}C^{18}O$ and ($Br_2 + Cl_2$) co-deposition experiments were also performed. Absorptions characterizing the two $^{12}C^{18}O$/BrCl complexes appeared at 2096.8_5 cm^{-1} and at 2087.0 cm^{-1} in the $\nu(^{12}C^{18}O)$ region. Figure 3 illustrates the infrared spectra of a typical experiment.

5.2. Nitrogen Matrix. The twin-jet co-deposition of diluted CO with Cl_2 into a nitrogen matrix (CO/N_2, 1/10000; Cl_2/N_2, 1/500) gave rise to a very sharp intense absorption at 2148.5 cm^{-1}. The same experiment with Br_2 gave results quite similar to that obtained from the Cl_2 experiment, namely, a sharp product absorption at 2152.5 cm^{-1}. The twin-jet co-deposition of a mixture of $Cl_2 + Br_2$ with CO led to the formation of three bands located at 2148.5, 2152.5, and 2156.9 cm^{-1}, as shown in Figure 4 in the ν(CO) region. They are assigned to $OC\cdots Cl_2$, $OC\cdots Br_2$, and $OC\cdots BrCl$ complexes, respectively. The existence of one band characterizing the interaction of CO with BrCl indicates that in the nitrogen matrix only one complex is preferentially formed, namely, $OC\cdots BrCl$. Another series of experiments was done with $^{13}C^{16}O$-enriched natural carbon monoxide co-deposited with Cl_2, Br_2, and then a mixture of ($Cl_2 + Br_2$). The three product bands were shifted to 2101.0, 2105.3, and 2109.6 cm^{-1}. Table 1 summarizes band positions for the product absorptions in this study.

6. Spectroscopic Trends and Structures of the Complexes

The magnitude of the blue shift of the perturbed CO stretching frequency is an indicator of the strength of the interaction of

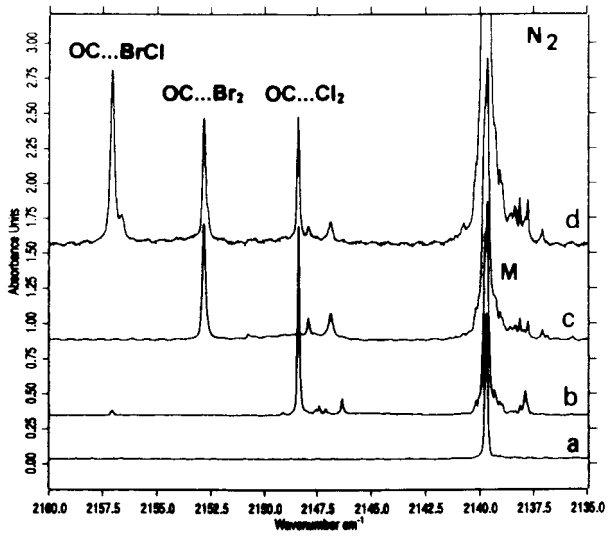

Figure 4. Comparison between IR spectra after deposition in the CO spectral region: (a) $CO/N_2 = 1/2000$ mixture; (b) $CO/Cl_2/N_2 = 1/10/10000$ mixture; (c) $CO/Br_2/N_2 = 1/10/10000$ mixture; (d) $CO/Cl_2 + Br_2/N_2 = 1/10 + 10/10000$ mixture.

TABLE 2: Comparison of Shifts $\Delta\nu$ for CO Molecule in Interaction with Cl_2, Br_2, and BrCl in Gas Phase and in Argon and Nitrogen Matrices[a]

	Cl_2···CO	Br_2···CO	ClBr···CO	BrCl···CO
gas	+6.2884	+9.57		
argon	+2.1	+5.4	+9.5	−0.5
nitrogen	+8.8	+12.8	+17.2	
calcd	+7.4	+10.6	+12.9	+5.8

[a] $\Delta\nu = \nu_0 - \nu_S$ (ν_0 is the frequency of the unperturbed molecule and ν_S the frequency of the perturbed molecule).

the two complexed partners. The shift increase from Cl_2 to BrCl indicates a stronger bonding in the OC···BrCl complex than in OC···Br_2 and OC···Cl_2. The OC···ClBr pair frequency nearly coincides with the CO monomer absorption.

The shift observed in the argon matrix when passing from Cl_2 to Br_2 of 3.3 cm^{-1} is comparable to that observed in the gas phase, which is 3.6 cm^{-1}. However, the blue shift from the uncomplexed monomer frequency is very different when changing from argon to nitrogen and from argon to the gas phase. Furthermore, no splitting due to different halogen isotopomers is observed in matrices. In the argon matrix the ν(CO) absorption of OC···Cl_2 is situated 2.1 cm^{-1} below the ν(CO) of monomer while it was found to be 6.28 cm^{-1} in gas phase and 8.8 cm^{-1} in nitrogen as summarized in Table 2. The strengthening of the interaction when coming from nitrogen to the argon matrix has been evident for other weak complexes[28] and has been explained by taking into account that in the nitrogen matrix solute molecules are subject to additional interactions with respect to the argon matrix.[29] Rare-gas matrices preserve generally the gas-phase structure, and frequencies in the argon matrix are often weakly shifted with respect to those in the gas phase, owing to a weak dynamic coupling between the complexes and the lattice vibration. Without questioning the gas-phase experimental results, it can be noted that the gas phase and matrix experimental conditions are very different. In the gas phase, the concentration of CO was very strong in regard to the Cl_2 concentration (Cl_2/CO/Ar: 1/30/300), whereas in our experiments, the CO concentration was very low. Thus, the formation of $(CO)_2$···Cl_2 complexes cannot be totally excluded. In the matrix, a temperature increase caused the appearance of a triplet at about 6 cm^{-1} below the CO monomer.

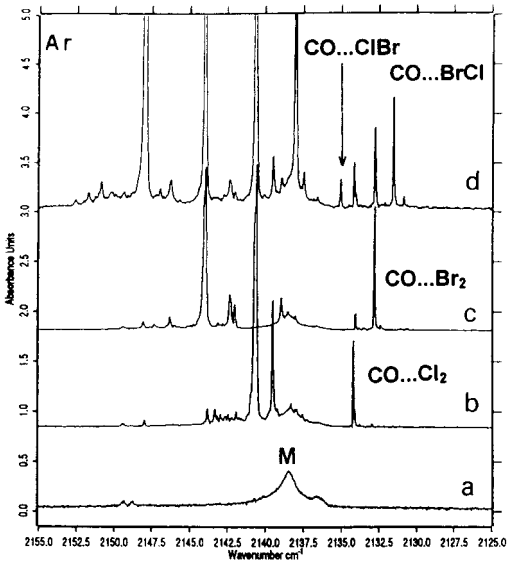

Figure 5. Infrared spectra in the ν(CO) spectral region recorded at 11 K after photolysis ($\lambda > 360$ nm) of X_2···CO complexes in the following matrices: (b) $CO/Cl_2/Ar = 1/4/2000$; (c) $CO/Br_2/Ar = 1/4/2000$; (d) $CO/Br_2 + Cl_2/Ar = 1/4 + 4/2000$. For comparison the spectrum of CO monomer in argon ($CO/Ar = 1/2000$) is shown trace a.

To our knowledge, only one study of complexes involving the BrCl molecule has been previously reported in the literature.[30] It concerned the interaction of BrCl with ozone in the argon matrix. Photodissociation study and calculations showed the existence of only one stable complex between ozone and bromine chloride in which ozone was bound to BrCl via the bromine atom. The existence of two 1:1 complexes between CO and BrCl isolated in solid argon and of only one complex in nitrogen shows that the nitrogen matrix modifies interactions in the complex.

7. Irradiation Effects. Identification of the CO···X_2 Species (Form 2)

After deposition of mixtures containing CO/Cl_2, CO/Br_2, or $CO/Cl_2 + Br_2$ in argon or nitrogen, the matrices were exposed to filtered radiation (cutoff filter, >360 nm) from a xenon lamp. In nitrogen matrices, spectra collected after irradiation were similar to those recorded after deposition, while in argon matrices new bands described below appeared.

As illustrated in Figure 5b, irradiation of the OC···Cl_2 complex formed from a $CO/Cl_2/Ar$ (1/5/2000) mixture led to the appearance of a new narrow band located at 2134.1 cm^{-1}, which disappeared with weak annealing. In the 1900−1800 and 900−800 cm^{-1} regions, very weak new doublets were measured at 1814−1813 and 840.3−839.3 cm^{-1}. They were assigned without ambiguity from the literature data[31] to the O═CCl_2 molecule.

When Cl_2 was subsituted by Br_2, a new band appeared at 2132.8 cm^{-1} in the ν(CO) region (Figure 5c). No other bands were observed in the lower frequency regions.

After irradiation of a $Cl_2 + Br_2$ mixture co-deposited with CO in argon (Figure 5d) the two bands at 2134.1 and 2132.8 cm^{-1}, which were observed previously, appeared with two new absorptions at 2131.5 and to 2135.1 cm^{-1}. The relative intensity of the four new absorptions was not clearly correlated to the relative intensity of the OC···X_2 precursor bands. It varied from one experiment to another and seemed to depend on the irradiation time, which was not exactly the same in all experiments. At lower frequency, doublets at 1819.3−1819.1

TABLE 3: Absorptions (cm^{-1}) Observed for the Perturbed Stretching Vibration (^{12}CO and ^{13}CO) in $CO\cdots Cl_2$, $CO\cdots Br_2$, $CO\cdots ClBr$, and $CO\cdots BrCl$ Trapped in Argon and Observed Shifts[a]

	$CO\cdots Cl_2$		$CO\cdots Br_2$		$CO\cdots BrCl$		$CO\cdots ClBr$	
	^{12}CO	^{13}CO	^{12}CO	^{13}CO	^{12}CO	^{13}CO	^{12}CO	^{13}CO
ν, cm^{-1}	2134.1	2087.1	2132.8	2085.8	2131.5	2084.6	2135.1	2088.0
$\Delta\nu_{obs}$, cm^{-1}	−4.4	−4.0	−5.5	−5.3	−7.0	−6.5	−3.3	−3.1
$\Delta\nu_{calc}$, cm^{-1}	−3.4	−3.3	−3.4	−3.4	−5.3	−5.1	−2.2	−2.2

[a] $\Delta\nu_{obs}$ (cm^{-1}) and calculated $\Delta\nu_{calc}$ (cm^{-1}) are from CO monomer absorption.

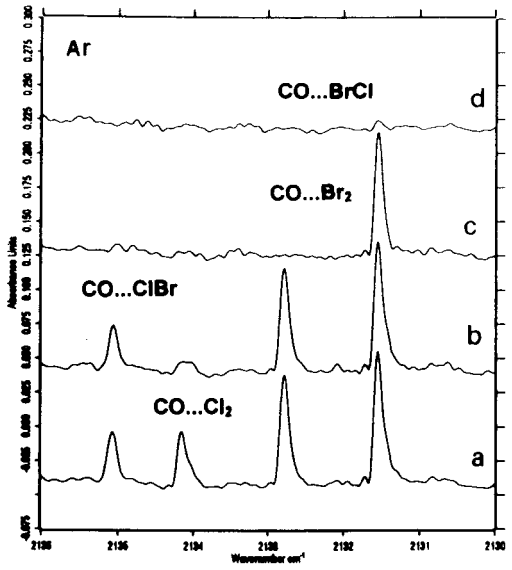

Figure 6. Temperature effects on the $CO\cdots X_2$ complexes formed after irradiation of a $CO/Cl_2 + Br_2/Ar = 1/10 + 10/10000$ mixture: (a) after deposition; (b) after annealing at 13 K; (c) after annealing at 15 K; (d) after annealing at 17 K. Spectra are recorded at 11 K.

and at 793.9−793.8 cm^{-1} were also observed. They are tentatively assigned to the formyl bromide chloride molecule (O═CBrCl) from its spectrum recorded in the gas phase.[32]

One experiment was carried out with a mixture of ^{13}CO and ($Cl_2 + Br_2$). Four bands appeared after irradiation. They were located at 2088.0, 2087.1, 2085.8, and 2084.6 cm^{-1}.

The new irradiation-induced bands at 2138.1, 2134.1, 2132.8, and 2131.5 cm^{-1}, located below the CO monomer absorptions, are assigned to complexes of form 2, namely, $CO\cdots ClBr$, $CO\cdots Cl_2$, $CO\cdots Br_2$, and $CO\cdots BrCl$ produced in very low yield from form 1 after irradiation. The red frequency shift of the submolecule CO in the $CO\cdots Cl_2$ complex is larger than the shift observed in the corresponding $OC\cdots Cl_2$ complexes as shown in Table 3, but the shift of the CO molecule when passing from Cl_2 to BrCl is smaller than in form 1 of complexes. A weak temperature increase that led to the disappearance of the $CO\cdots X_2$ complexes indicates that the $CO\cdots X_2$ form is less stable than the $X_2\cdots CO$ form. However, back isomerization of the $CO\cdots X_2$ complexes by infrared irradiation was not observed, suggesting that they isomerize in the same wavelength range as that of the $X_2\cdots CO$ complexes to produce a photochemical equilibrium. An interesting observation of Figure 6, which compares the temperature effect on the evolution of the four $CO\cdots X_2$ complexes, can be made. It can be seen that the $CO\cdots Cl_2$ complex disappears at 13 K, while $CO\cdots Br_2$ and $CO\cdots ClBr$ disappear at 15 K and $CO\cdots BrCl$ vanishes at 17 K, indicating the different stabilities of these complexes. Further experiments of the kinetics of the appearance of the $CO\cdots X_2$ complexes at various wavelengths and their disappearance at different temperatures will be carried out, and results will be reported in a forthcoming paper.

Formation of the $CO\cdots X_2$ complexes occurs probably from isomerization of the $OC\cdots X_2$ complexes by a rotation of the CO molecule. Such a behavior was observed for hydrogen-bonded complexes involving HI as a proton donor [ref 33 and references therein]. The hydrogen-bonded forms were infrared-photodissociated into weakly interacting van der Waals pairs but were regenerated by warming the matrix. Ab initio calculations suggested that the conversion was due to the head-to-tail change in the orientation of HI relative to the base molecule.[34]

The observation of traces of $COCl_2$ after irradiation shows that the photochemistry of the $Cl_2\cdots CO$ complex is different from that of each partner. At $\lambda > 360$ nm the isolated Cl_2 molecule is not dissociated, whereas in the complex it is. Formation of $COCl_2$ occurs probably by simultaneous dissociation of Cl_2 and transfer of one Cl atom to the carbon atom followed by the attachment of the other chlorine atom upon the carbon atom, as assumed by the following scheme:

$$Cl\text{-}Cl\cdots CO \rightarrow [Cl\cdots Cl\text{-}C{=}O] \rightarrow \begin{matrix} Cl \\ \diagdown \\ C{=}O \\ \diagup \\ Cl \end{matrix}$$

The same trend was observed for the $ClBr\cdots CO$ complex but not for the $Br_2\cdots CO$ complex probably because of the size of the Br atom, which prevents the migration on the carbon atom of the bromine atom in the second step of the process. Isomerization of the $X_2\cdots CO$ complex in nitrogen was not observed. The nitrogen matrix stabilizes the complex or hinders the rotation of CO.

8. Calculations. Results and Discussion

Calculated properties of isolated species are displayed in Table 4. The geometry, at the B3LYP level, and absolute energies at the B3LYP, CCSD/B3LYP, and CCSD(T)/B3LYP levels are displayed in Table 5 for Cl_2 and Br_2 complexes and in Table 6 for BrCl complexes (forms 1 and 2). Previous calculations on $Cl_2\cdots CO$ and $CO\cdots Cl_2$ complexes by Bunte et al.[15] have shown that only linear complexes are stable enough to allow their trapping. We thus limited ourselves to those complexes. Nevertheless, all the parameters were independently optimized. Indeed, the resulting geometries exhibit meaningless deflections from linearity (ca. 1°), which have not been reported. Calculated frequency shifts of CO are reported beside the experimental values in Tables 2 and 3. Finally, the stabilization energies are collected in Table 7. The intermolecular bonding distances, in the 3−3.5 Å range, correspond to van der Waals interactions. In the case of $Cl_2\cdots CO$, its value (3.097 Å) is very close to Bunte's value, namely, 3.1 Å, but a greater interaction distance is found for $Cl_2\cdots OC$ (3.255 Å), in disagreement with the value from this study (3.06 Å). Taking into account that in all complexes the C interactions result in shorter distances than O interactions, this result seems consistent with the greater energy of the C interaction with respect to the O interaction. Table 7 shows that the B3LYP and CCSD(T) give comparable stabilization energies for C-interacting complexes, but B3LYP

TABLE 4: Calculated Properties of Isolated CO, Cl_2, Br_2, and BrCl[a]

CO		C−O	*E*	dipole	ν(CO)
	B3LYP	1.124 866	−113.362 526	0.1070	2215.01 (76)
	CCSD/B3LYP		−113.142 252		
	CCSD(T)/B3LYP		−113.158 863		
Cl_2		Cl−Cl	*E*	dipole	ν(Cl)
	B3LYP	2.024 725	−920.417 514	0.0	537.75 (0)
	CCSD/B3LYP		−919.388 142		
	CCSD(T)/B3LYP		−919.405 381		
Br_2		Br−Br	*E*	dipole	ν(Br)
	B3LYP	2.393 805	−5148.336 832	0.0	286.11 (0)
	CCSD/B3LYP		−5145.185 191		
	CCSD(T)/B3LYP		−5145.195 240		
BrCl		Br−Cl	*E*	dipole	ν(BrCl)
	B3LYP	2.184 505	−3034.379 993	0.5674	421.23 (0.83)
	CCSD/B3LYP		−3032.296 415		
	CCSD(T)/B3LYP		−3032.309 947		

[a] Bond lengths in Å, absolute energies in au, vibrational frequency in cm^{-1}, and band intensity in parentheses.

TABLE 5: Calculated Properties of CO···Cl_2 and CO···Br_2 Complexes (See Caption of Table 4)

species		B3LYP	CCSD/B3LYP	CCSD(T)/B3LYP	$\Delta\nu$(CO)	$\Delta\nu$(X−X)
O−C···Cl−Cl	CO	1.124				
	ClC	3.097				
	ClCl	2.030				
	μ	0.006 98				
	energy	−1033.781 541	−1032.531 958	−1032.566 280	+7.4	−10.1
C−O···Cl−Cl	CO	1.125				
	ClO	3.255				
	ClCl	2.025				
	μ	0.0630				
	energy	−1033.780 480	−1032.531 476	−1032.565 494	-3.3_5	−0.72
O−C···Br−Br	CO	1.124				
	CBr	3.094				
	BrBr	2.404				
	μ	0.9302				
	energy	−5261.701 114	−5258.328 581	−5258.355 732	+10.6	−9.6
C−O···Br−Br	CO	1.125				
	BrO	3.477				
	BrBr	2.394				
	μ	0.0760				
	energy	−5261.699 767	−5258.328 318	−5258.355 079	−3.4	−0.3

TABLE 6: Calculated Properties of CO···BrCl Complexes (See Caption of Table 4)

species		B3LYP	CCSD/B3LYP	CCSD(T)/B3LYP	$\Delta\nu$(CO)	ν(X−Y)
O−C···Cl−Br	CO	1.124				
	ClO	3.203				
	ClBr	2.189				
	μ	0.0495				
	energy	−3147.743 505	−3145.439 768	−3145.470 266	+5.8	414.03 (0.5)
C−O···Cl−Br	CO	1.125				
	ClO	3.382				
	ClBr	2.185				
	μ	0.5378				
	energy	−3147.742 787	−3145.439 568	−3145.469 862	−2.2	420.96 (0.3)
O−C···Br−Cl	CO	1.123				
	BrC	3.042				
	BrCl	2.193				
	μ	0.9302				
	energy	−3147.745 008	−3145.440 643	−3145.471 346	+12.9	409.05 (9.5)
C−O···Br−Cl	CO	1.1255				
	BrO	3.350				
	BrCl	2.185				
	μ	0.6827				
	energy	−3147.743 248	−3145.440 014	−3145.470 267	−5.3	420.18 (1.8)

appears to underestimate O-interaction energies. BSSE corrections do not modify the qualitative trends observed for CO···Cl_2 and CO···ClBr complexes; the stabilization energies are lowered by ca. 30−40%. Nevertheless, they drop dramatically in the case of CO···Br_2 complexes. It could be an artifact of the method, which is only a crude estimate of the correction. ZPE corrections have been calculated using B3LYP frequencies. Their values are in the range 0.44−0.18 kcal mol^{-1}, and they

TABLE 7: Stabilization Energies (kcal) of Complexes at Various Calculation Levels[a]

	B3LYP	CCSD	CCSD(T)	CCSD(T)[b]	BSSE	ref 15[c]
O−C···Cl−Cl	0.94	0.98	1.28	0.84	0.83	1.58 (1.23)
C−O···Cl−Cl	0.28	0.68	0.78	0.56	0.55	0.96 (0.66)
O−C···Br−Br	1.10	0.71	1.02	0.80	0.27	
C−O···Br−Br	0.26	0.55	0.61	0.43	0.05	
O−C···Cl−Br	0.62	0.69	0.91	0.56	0.51	
C−O···Cl−Br	0.17	0.57	0.66	0.44	0.44	
O−C···Br−Cl	1.56	1.24	1.59	1.13	0.76	
C−O···Br−Cl	0.46	0.85	0.91	0.65	0.56	

[a] BSSE corrections are performed at the CCSD(T) level. [b] ZPE-corrected values using B3LYP frequencies. [c] Values in parentheses refer to BSSE-corrected energies.

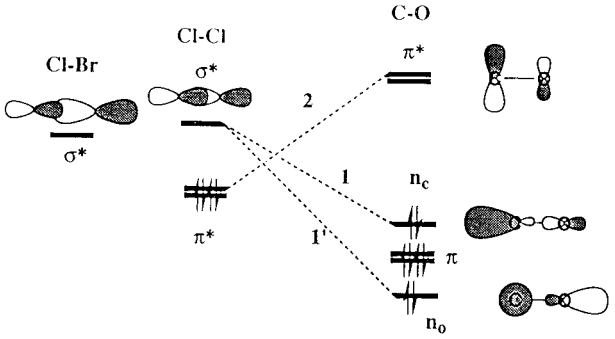

Figure 7. Qualitative MO perturbation scheme of dihalogen and carbon monoxide molecules.

are not negligible. CCSD(T) stabilization energies after ZPE correction given in Table 7 show that the relative energies remain almost unchanged. The calculated frequency shifts (Tables 2 and 3) are generally in good agreement with nitrogen matrix experimental values; once taken into account, this matrix seems to increase these values by ca. 30% with respect to the gas phase. It strongly supports the preceding assignments. Nevertheless, in the only case of BrCl···CO, the experimental red shift of -0.5 cm^{-1} (argon) disagrees with the calculated blue shift of 5.8 cm^{-1} as well as the blue shift measured experimentally for other complexes so that the actual nature of this species can be questioned. In the case of the BrCl···CO complex, the calculated shift is weaker than for the Cl_2···CO complex, and this is in good agreement with experimental results in argon.

Though the interaction between carbon monoxide and dihalogens results from a balance of several terms, it is worthy to note that the main trends in the preceding results, and especially in frequency shifts, can be understood by a simple MO perturbation scheme, displayed in Figure 7 in the case of Cl_2. Charge transfer can a priori occur either from CO to Cl_2 via a σ overlap (interactions 1 and 1′) or from Cl_2 to CO via a π overlap (interaction 2). The latter interaction is expected to be almost negligible, since at these interaction distances the π overlap is very weak. Moreover, this interaction would result in any case in a weakening of the CO bond, especially in C-bonded complexes that involve a larger π overlap, and cannot explain the blue shift observed for these species. In C-bonded complexes, the main MO interaction is thus interaction 1, in which the electron density is transferred from the carbon lone pair MO, n_C, to σ^* of halogen. In fact, n_C is not purely nonbonding but bears some CO antibonding character so that the electron-transfer strengthens the CO bond, in agreement with the blue shift in vibration frequency. The reverse result is observed in O-bonded complexes involving 1′ as the main interaction, since n_O bears some bonding character; this effect is weaker than the preceding one because of the greater $n_O-\sigma^*$ energy gap with respect to the $n_C-\sigma^*$ one. In fact, the bonding/antibonding character of n_O and n_C is not easily stated by a simple examination of the AOs coefficients but can be evidenced by CO stretching; in this case the energy of n_C is lowered, whereas the energy of n_O is raised. This interaction scheme is supported by the observed CO-to-Cl_2 charge transfer of ca. 10^{-2} electron for C complexes and 10^{-3} electron for O complexes. In the latter case, nevertheless, this transfer is so weak that the bonding should involve other interactions, especially through electrostatic quadrupoles and dispersion. This scheme is also consistent with the influence of the bonded halogen site; the interaction is expected to increase with its electrophilic character, which depends on the level of σ^*, on the relative AO coefficients, and on the net charge for the dissymmetrical ClBr. The greater electrophilic character is thus encountered for Br in Br−Cl, enhanced by the polarization of the molecule, and the less electrophilic one for Cl in BrCl. The absolute shift in frequencies in argon is found to decrease with the halogen electrophilic character in the sequence Br−(Cl) > Br−(Br) > Cl−(Cl) > Cl−(Br).

Acknowledgment. Computations were performed on a RS6000 workstation at the "Institut de Développement des Ressources Informatiques Scientifiques" (IDRIS, Orsay, France). The authors thank Dr. J. Leszczynski for reading the manuscript.

References and Notes

(1) Schriver, D. F.; Atkins, P. W.; Langford, C. H. *Inorganic Chemistry*; Freeman W. H.: San Francisco, 1990; p 66.
(2) D'Amico, K. L.; Trenary, M.; Shinn, N. D.; Solomon, E. I.; McFeely, F. R. *J. Am. Chem. Soc*. **1982**, *104*, 5102.
(3) Benzel, M. A.; Dykstra, C. E. *Chem. Phys*. **1983**, *80*, 273; *J. Chem. Phys*. **1984**, *80*, 3510.
(4) Slanina, Z. *Thermochim. Acta* **1986**, *10*, 287.
(5) Curtiss, L. A.; Pochatko, D. J.; Reed, A. E.; Weinhold, F. *J. Chem. Phys*. **1985**, *82*, 2679.
(6) Soper, P. D.; Legon, A. C.; Flygare, W. H. *J. Chem. Phys*. **1981**, *74*, 2138.
(7) Wang, Z.; Bevan, J. W. *Chem. Phys. Lett.* **1989**, *161*, 6.
(8) Wang, Z.; Bevan, J. W. *Chem. Phys. Lett.* **1990**, *167*, 49.
(9) Suckeley, A.; Legon, A. C.; Wang, Z.; Bandarage, G.; Lucchese, R. R.; Bevan, J. W. *J. Chem. Phys*. **1993**, *98*, 1761.
(10) McKellar, A. R. W.; Zeng, Y. P.; Sharpe, S. W.; Wittig, C.; Beaudet, R. A. *J. Mol. Spectrosc*. **1992**, *153*, 475.
(11) Andrews, L.; Arlinghaus, R. T.; Johonson, G. L. *J. Chem. Phys*. **1983**, *78*, 6347.
(12) Schatte, G.; Willner, H.; Hodge, D.; Knözinger, E.; Schrems, O. *J. Phys. Chem*. **1989**, *93*, 6025.
(13) Bunte, S. W.; Miller, J. B.; Huang, Z. S.; Verdasco, J. E.; Wittig, C.; Baudet, R. A. *J. Phys. Chem*. **1992**, *96*, 41408. Otaga, T.; Jäger, W.; Ozier, I.; Gerry, M. C. L. *J. Chem. Phys*. **1993**, *98*, 9399.
(14) Lin, Y.; Baudet, R. A. *J. Phys. Chem*. **1994**, *98*, 8310.
(15) Bunte, S. W.; Chabalowski, C. F.; Wittig, C.; Beaudet, R. A. *J. Phys. Chem*. **1993**, *97*, 5864.
(16) Raducu, V.; Jasmin, D.; Dahoo, R.; Brosset, P.; Gauthier-Roy, B.; Abouaf-Marguin, L. *J. Chem. Phys*. **1995**, *102*, 9235.
(17) Frisch, M. J.; Trucks, G. W.; Schlegel, H. B.; Gill, P. M. W.; Johnson, B. G.; Robb, M. A.; Cheeseman, J. R.; Keith, T.; Petersson, G. A.; Montgomery, J. A.; Raghavachari, K.; Al-Laham, M. A.; Zakrzewski, V. G.; Ortiz, J. V.; Foresman, J. B.; Cioslowski, J.; Stefanov, B. B.;

Nanayakkara, A.; Challacombe, M.; Peng, C. Y.; Ayala, P. Y.; Chen, W.; Wong, M. W.; Andres, J. L.; Replogle, E. S.; Gomperts, R.; Martin, R. L.; Fox, D. J.; Binkley, J. S.; Defrees, D. J.; Baker, J.; Stewart, J.; Head-Gordon, M.; Gonzalez, C.; Pople, J. A. *Gaussian 94*, revision B.1; Gaussian Inc.: Pittsburgh, PA, 1995.

(18) Chaquin, P.; Bahou, M.; Schriver-Mazzuoli, L.; Schriver, A. *Chem. Phys. Lett.* **1996**, *256*, 609.

(19) Hallou, A.; Schriver-Mazzuoli, L.; Schriver, A.; Chaquin, P. *Chem. Phys*. **1998**, *237*, 251.

(20) Lee, T. J. *J. Phys. Chem*. **1995**, *99*, 15074.

(21) Becke, A. D. *J. Chem. Phys*. **1993**, *98*, 5648.

(22) Lee, C.; Yang, W.; Paar, R. G. *Phys. Rev*. **1988**, *B37*, 785. Mielich, B.; Savin, A.; Stall, H.; Preuss, H. *Chem. Phys. Lett*. **1989**, *157*, 200.

(23) Schaefer, A.; Huber, C.; Ahlrichs, R. *J. Chem. Phys*. **1994**, *100*, 5829.

(24) Dubost, H.; Abouaf-Marguin, L. *Chem. Phys. Lett.* **1972**, *17*, 269.

(25) Diem, M.; Tso, T.-L.; Lee, E. K. C. *Chem. Phys*. **1982**, *73*, 283.

(26) Lundell, J.; Rasanen, M. *J. Phys. Chem*. **1995**, *99*, 14301.

(27) Nelander, B. *J. Phys. Chem*. **1985**, *89*, 827.

(28) Schriver-Mazzuoli, L.; Schriver, A.; Wierzejewska-Hnat, M. *Chem. Phys*. **1995**, *199*, 227.

(29) Perchard, J. P.; Maillard, D.; Schriver, A.; Girardet, C. *J. Raman Spectrosc*. **1981**, *11*, 406.

(30) Bahou, M.; Schriver-Mazzuoli, L.; Schriver, A.; Chaquin, P. *Chem. Phys*. **1997**, *216*, 105.

(31) Bouteiller, Y.; Abdelaoui, O.; Schriver, A.; Schriver-Mazzuoli, L. *J. Chem. Phys*. **1995**, *102*, 1731.

(32) Schriver-Mazzuoli, L.; Schriver, A.; Perchard, J. P. *J. Mol. Struct*. **1990**, *222*, 141.

(33) Hannachi, Y.; Silvi, B.; Perchard, J. P. *Chem. Phys*. **1991**, *154*, 23.